

Isolation and identification of senescent renal tubular epithelial cells using immunomagnetic beads based on DcR2



Jia Chen, Ke-Hong Chen, Bi-Qiong Fu, Weiwei Zhang, Huanzi Dai, Li-Rong Lin, Li-Ming Wang, Ya-Ni He *

Department of Nephrology, Daping Hospital, Third Military Medical University, Chongqing, China

ARTICLE INFO

Article history:

Received 10 December 2016

Received in revised form 21 April 2017

Accepted 21 April 2017

Available online 28 April 2017

Keywords:

Cell senescence

Renal tubular epithelial cell

Cell sorting

Decoy receptor 2

ABSTRACT

Cell senescence plays a major role in the progression of tumors and chronic conditions such as diabetes and chronic kidney disease. Senescent cells are an important model for the study of aging-related diseases, and there is currently no efficient method for sorting out senescent cells. Decoy receptor 2 (DcR2) is a transmembrane receptor of the tumor necrosis factor superfamily, which is specifically expressed in senescent cells. In this study, we used magnetic activated cell sorting (MACS) isolation of a highly-pure populations DcR2-positive renal tubular epithelial cells (RTECs) based on three senescent cell models including the fifth passage cells, advanced glycation end-products (AGEs)- and H₂O₂-induced cells. The percentages of DcR2 positive RTECs in G1 and S phases increased by 20% and 4%, respectively, as compared to that in the pre-sorted cells. The positivity rates of SA-β-gal, p16, and senescence-associated heterochromatin foci (SAHF) in DcR2-positive RTECs were about 40%, 30%, and 44% higher than that prior to cell sorting. The levels of IL-6 and TGF-β1 in the supernatant were increased by 1.7 and 1.5 folds, respectively, as compared to that observed prior to sorting. No significant cell death was observed after 5 days of continuous culture. Ki-67 positive expression rate in DcR2 negative RTECs was significantly higher than that in DcR2 positive RTECs after MACS. We demonstrated the use of DcR2 to classify live, senescent RTECs with a high specificity and stability. Our findings lay the foundation for further study of senescent RTECs in the progression of chronic kidney disease.

© 2017 Elsevier Inc. All rights reserved.

1. Introduction

Progressive population aging is associated with a concomitant increase in economic and social burden of age-related diseases such as chronic kidney disease (CKD), diabetes mellitus, Alzheimer's disease and cancers (Harper 2014). Aging is a complex phenomenon that involves changes at both the organismal and cellular level (Matjusaitis et al. 2016). Cell senescence refers to the permanent loss of proliferative and regenerative ability brought about by irreversible cell cycle arrest (Hayflick 1965). Senescent cells are resistant to stress injury and self-repair ability. Further, senescent cells promote aging of normal tissue cells and are also implicated in the development of aging-related diseases through the release of inflammatory factors, chemokines and other senescence-associated secretory phenotypes (SASP) (Freund et al. 2010; Munoz-Espin and Serrano 2014; Salama et al. 2014). Therefore, senescent cell is an important model for the study of the pathogenesis of aging-related diseases. However, current methods for sorting of senescent cells have several shortcomings. Fluorescence-based cell sorting (FACS) technology has been used to isolate relatively pure senescent

cells based on cell size and lipofuscin content. However, the high-pressure conditions of flow cytometry tend to have a detrimental effect on the biology of the isolated senescent cells (Hewitt et al. 2013). Similarly, the microfluidic filter used for sorting of senescent cells based on the cell diameter lacks specificity (Kim et al. 2015). Magnetic affinity cell sorting (MACS) can be used to obtain highly pure target cells by binding of immunomagnetic beads with cell membrane markers, and without incurring cell damage (Zhang et al. 2015). The use of immunomagnetic beads based on membrane markers may be a viable technique for sorting of senescent cells.

Decoy receptor 2 (DcR2), a transmembrane receptor for tumor necrosis factor superfamily, plays an anti-apoptotic role after binding to the tumor necrosis factor superfamily ligand TRAIL (Kimberley and Sreaton 2004). DcR2 is highly expressed in senescent cells and has been used as a marker for aging tumor cells (Collado et al. 2005). The expression of DcR2 in senescent fibroblasts was shown to be closely related to the degree of hepatic fibrosis (Sagiv et al. 2013). Moreover, expression of DcR2 in senescent tumor cells has been used to assess tumor differentiation as well as for evaluation of therapeutic efficacy (Macher-Goepfing et al. 2009; Vindrieux et al. 2011). Renal tubular epithelial cell (RTEC) senescence provides one of the most senile parenchymal cells in kidney disease, which are closely related to kidney disease progression (Liu et al. 2012; Satriano et al. 2010; Verzola et al.

* Corresponding author at: Department of Nephrology, Daping Hospital, Third Military Medical University, Chongqing 400042, China.
E-mail address: hey@mail@163.com (Y.-N. He).

2008). Whether DcR2 is highly expressed in senescent RTECs, and whether MACS based on DcR2 can be used to obtain stable and viable form of actively senescent RTECs, is not clear.

In our preliminary study, the expression of DcR2 in the cytomembrane and cytoplasm of RTECs was found to be significantly increased in the aging model. In the present study, we aimed to obtain DcR2-positive RTECs with use of MACS method; the morphology, cell cycle, and senescent phenotypes were tested to assess the use of this approach for isolation of stable and specific senescent RTECs. Further, the viability and proliferation capacity of DcR2-positive and -negative RTECs were also assessed to determine the effect of this method on cell viability.

2. Materials and methods

2.1. Materials and reagents

Dulbecco's modified Eagle's medium/F-12 (DMEM/F-12), fetal bovine serum (FBS), penicillin/streptomycin, RIPA, PMSF, PVDF membrane; type II collagenase and trypsin (Hyclone, USA); anti-rabbit IgG immunomagnetic beads (Cat. No. 130-048-062, Miltenyi, Biotec, Bergisch Gladbach, Germany); primary antibodies including DcR2 (rabbit monoclonal, Cat. No. ab108421, Abcam, Cambridge, UK); P16 (mouse monoclonal, Cat. No. ab54210, Abcam, Cambridge, UK); FLIP (mouse monoclonal, Cat. No. ab81617, Abcam, Cambridge, UK); caspase-3 (mouse monoclonal, Cat. No. sc56053, Santa Cruz Biotechnology, Heidelberg, Germany); Ki-67 (mouse monoclonal, Cat. No. BM2889, Boster, Wuhan, China); GAPDH (mouse monoclonal, Cat. No. AG019, Biyuntian, Shanghai, China); secondary antibodies including IgG (goat anti-rabbit polyclonal, Cat. No. ab150077), FITC (goat anti-mouse polyclonal, Cat. No. ab6785) and CY3 (goat anti-rabbit polyclonal, Cat. No. ab6939) from Abcam, Cambridge, UK. DAPI working solution, cell cycle kit and SA- β -Gal kit (Biyuntian, Shanghai, China); Conventional

chemical reagents such as glucose, H₂O₂, bull serum albumin (BSA) (Sigma-Aldrich, St. Louis, MO, USA).

2.2. Cell culture and treatment

The renal cortical tissue of 3-week-old male C57/BL6 mice was obtained under sterile conditions. Type II collagenase was used to digest the renal cortex, and the primary RTEC sieved, isolated and cultured (Terry et al. 2007). The second-passage RTECs were inoculated in a 10 cm culture dish and served as the normal control group. The same volume of second passage of the RTEC suspension was induced in 10 cm culture dishes by advanced glycation end-products (AGEs) (7.5 μ mol/L) for 48 h, and H₂O₂ (0.3 mmol/L) for 3 h. After 3 h of induction, the cells were washed twice with PBS and cultured in normal medium for 48 h. In addition, the primary RTEC was passaged for the fifth passage to construct three senescent RTEC models (Liu et al. 2014; Satriano et al. 2010). The morphology of the cells was observed under an inverted microscope.

2.3. MACS

The single cell suspensions were prepared from every 10 cm culture dish and resuspended after centrifugation at 1500 rpm for 5 min. Subsequently, DcR2 antibody (dilution 1:100) was added to single cell suspensions and the mixture was incubated at 4 °C for 1 h and washed twice with a buffer (phosphate buffered saline solution containing 0.5% BSA and 2.0 mmol/L EDTA, pH 7.2). Half of the cell suspension was incubated with FITC for detection of DcR2 positive expression and cell counting; the other half of cells were incubated again after addition of 20 μ L of immunomagnetic beads per 10⁷ cells at 4 °C for 15 min on a rotator (Miltenyi, Biotec, Bergisch Gladbach, Germany), washed twice with buffer and resuspended after centrifugation at 1500 rpm for

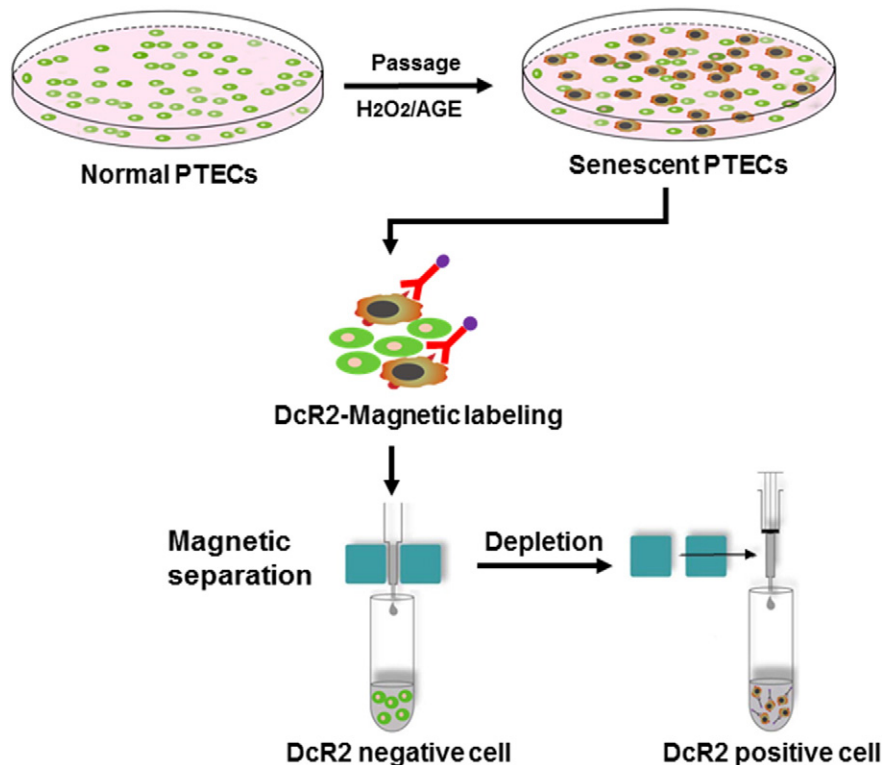


Fig. 1. DcR2-positive cell sorting pattern using MACS.

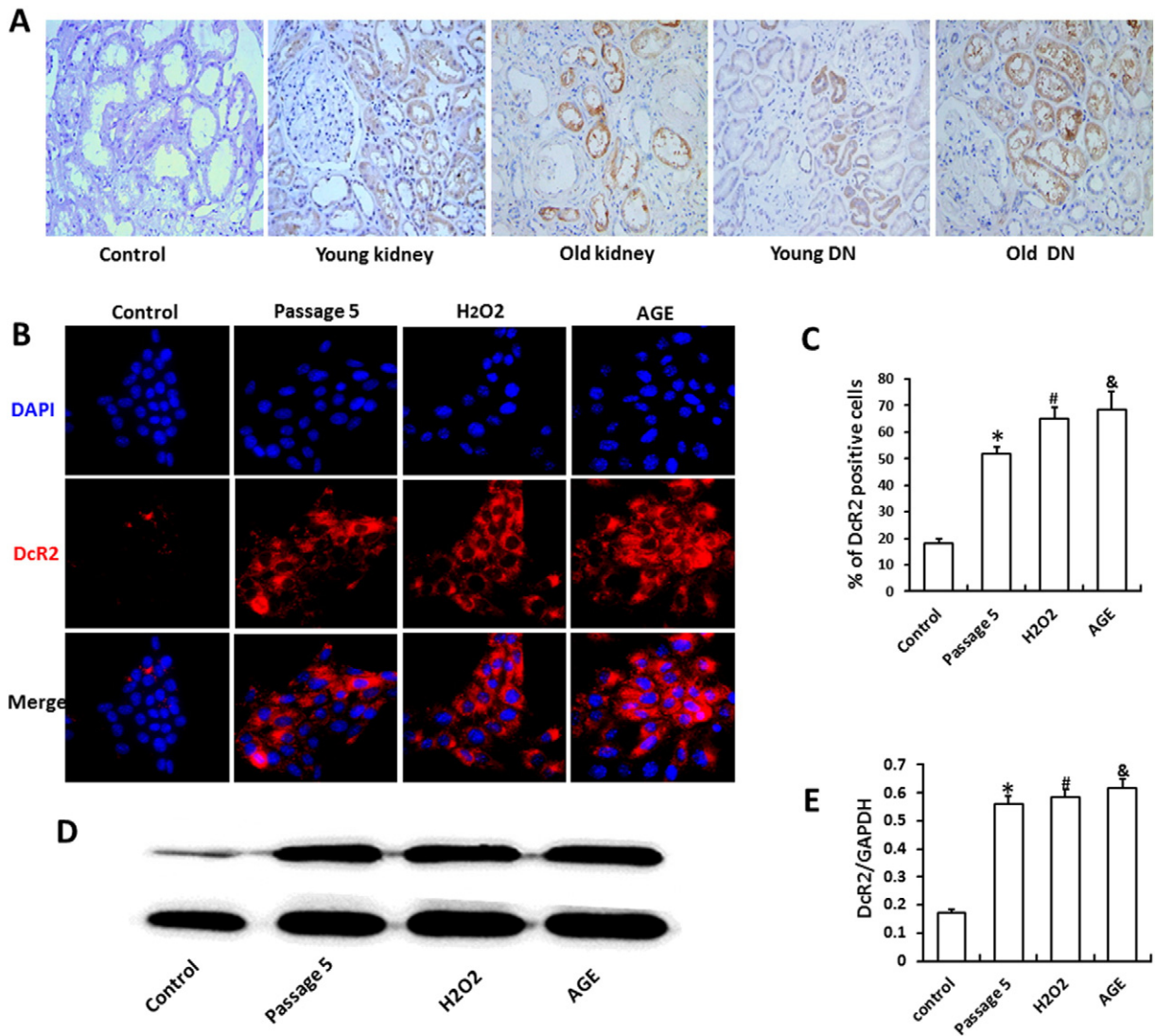


Fig. 2. Expressions and distribution of DcR2-positive RTECs in renal tissue and in various senescent model groups. (A) Expression and distribution of DcR2 in old and young renal tissues; (B–C) Immunofluorescence staining of RTEC DcR2 in control and senescent model groups (magnification, $\times 600$); (D–E) Western blot analysis of RTEC DcR2 in each group. */#/& $P < 0.05$, vs. control.

5 min. Prior to cell sorting, the cells were counted with a cell count plate. The cell count was approximately 1×10^6 from every senescent model. The pre-sorted cell suspensions were added to the LS column on the midiMACS separator (Miltenyi, Biotec, Bergisch Gladbach, Germany) after addition of 3 mL buffer wetting LS. The immunomagnetic bead sorting column was then washed three times with 3 mL of buffer, and the collected cells were DcR2-negative RTECs (unlabeled cells). After removing the LS column from the midiMACS separator and placing it on a suitable tube, 5 mL of buffer was immediately added, the piston pushed vigorously and the LS column washed and rinsed twice. The collected cells were DcR2 positive RTECs (labeled cells); the cell count was found to be approximately 5×10^5 with the cell counting plate from every senescent model (Fig. 1).

2.4. Immunohistochemistry and Immunofluorescence

Expression of DcR2 in renal tissue was detected by a 2-step immunohistochemical staining technique. All specimens were deparaffinized and rehydrated. Following antigen retrieval, tissues were treated with monoclonal primary anti-DcR2 antibody (dilution 1: 200) and

incubated at 4 °C overnight. After rinsing in PBS, the samples were stained with horseradish peroxidase-conjugated anti-mouse or anti-rabbit IgG for 30 min at 37 °C. After the last PBS wash, the sections were incubated with DAB reagent. Furthermore, the cell climbing tablets were fixed and closed with serum, anti-DcR2, anti-P16, anti-Ki67, anti-FLIP and anti-caspase-3 (dilution 1: 100) were incubated overnight at 4 °C, and the anti-CY3-labeled goat anti-rabbit IgG and FITC-labeled goat anti-mouse IgG were added drop-wise. Then, the tablets were incubated at 37 °C for 1 h. EVOS fluorescence microscope was used for imaging and observation of chart. Six visual fields were randomly selected to calculate the percentage of positively stained cells in the total RTECs.

Protein extraction and western blot analysis

The appropriate amount of lysis solution was added to the ice lysis cells for 10 min and centrifugated at 4 °C at 12000 rpm for 15 min. After preparing adhesive and concentrated gel with an appropriate concentration loading, electrophoresis, and transferring membrane were gone on according to the kit instructions. After blocking with 5% defatted milk at room temperature for 2 h, the membrane was

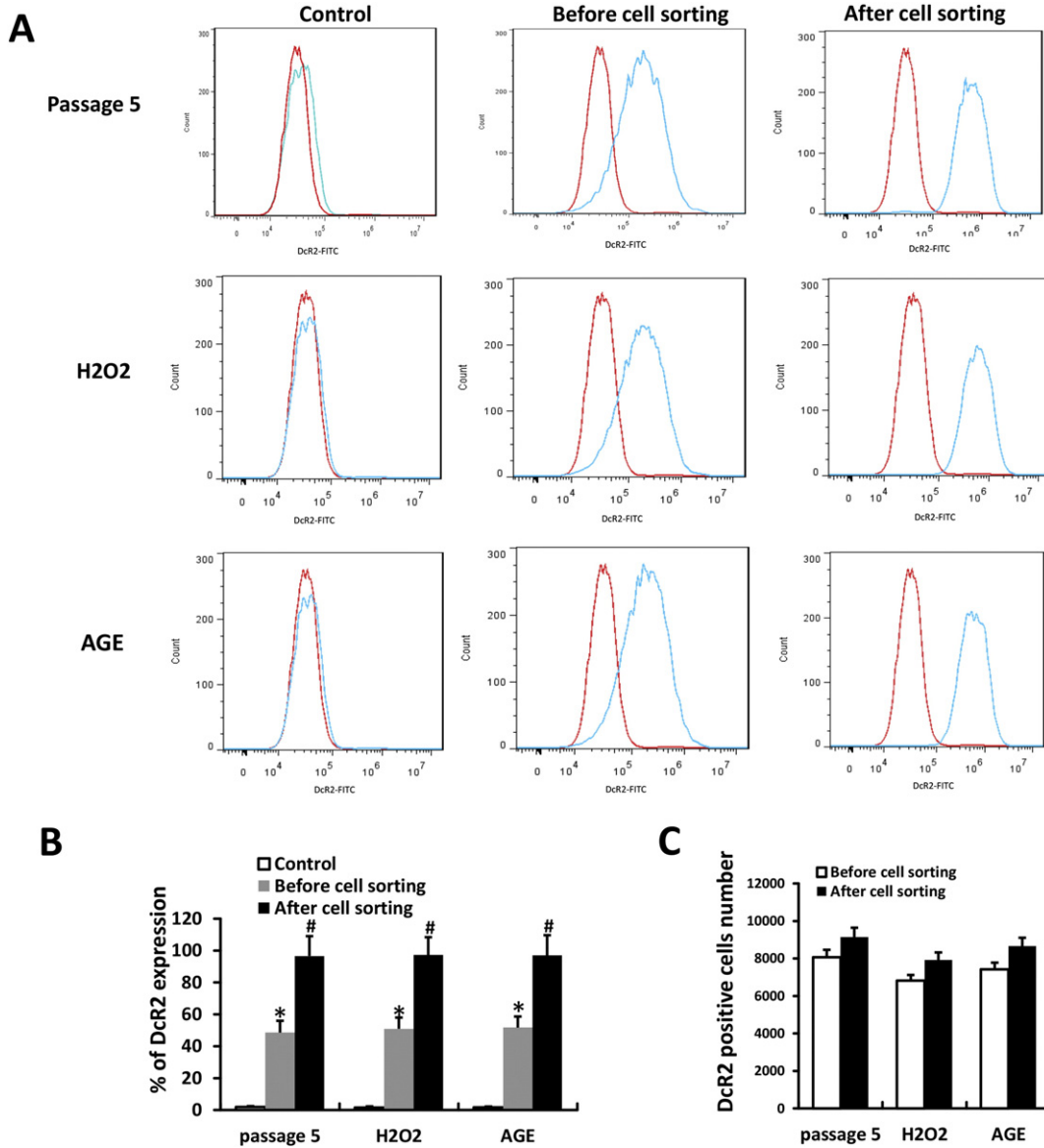


Fig. 3. The percentage of DcR2 surface expression and the number of DcR2 positive cells analyzed by flow cytometry. (A–B) Representative histogram and the percentage of cells with DcR2 surface expression in senescent models before and after sorting. Control antibody is indicated by red line. Data presented as mean ± SD (n = 3) (*P < 0.05 vs. control; # P < 0.05 vs. before cell sorting). (C) The numbers of DcR2 positive cells prior to and after sorting.

incubated overnight at 4 °C with DcR2 antibody (dilution 1: 2000) and GAPDH (dilution 1: 2000). The membranes were incubated with horseradish peroxidase-conjugated secondary antibodies for 1 h at room temperature. Immunoblots were developed with ECL detection system and analyzed using Quantity One software.

2.6. Flow cytometric analysis

The cells were pelleted and washed twice with cold PBS and fixed with 70% ethanol for 12 h at 4 °C. The immobilized cells were washed twice with cold PBS and stained with 50 µg/mL PI for 30 min. The cell cycle was detected by flow cytometry (BD Biosciences). In addition, the cells obtained before and after sorting were washed with standard buffer (PBS, 2% BSA) incubated for 60 min at 4 °C with DcR2 antibodies, then the FITC-labeled goat anti-rabbit IgG were incubated for 10 min at 4 °C. Cells were washed three times with standard buffer; then the same volume of cells were analyzed by flow cytometer (BD Biosciences). The

percentages of cells in G1/S phases, expression of DcR2 and the number of DcR2 positive cells were analyzed by FlowJo Version 7.6.1 software (TreeStar).

2.7. SA-β-Gal staining

The SA-β-Gal fixative was used to fix the cells according to the manufacturer's instructions. The staining solution was incubated at 37 °C overnight and observed under a light microscope. The cytoplasm of SA-β-Gal in positive RTEC showed a bright blue color, and the percentage of such cells in total RTECs was calculated.

2.8. Senescence-associated heterochromatin foci (SAHF) analysis

The cells were fixed, and the DAPI solution was added dropwise. The SAHF accumulation was observed under a Delta Vision fluorescence microscope. Six high power fields were randomly selected and 15–20 cells

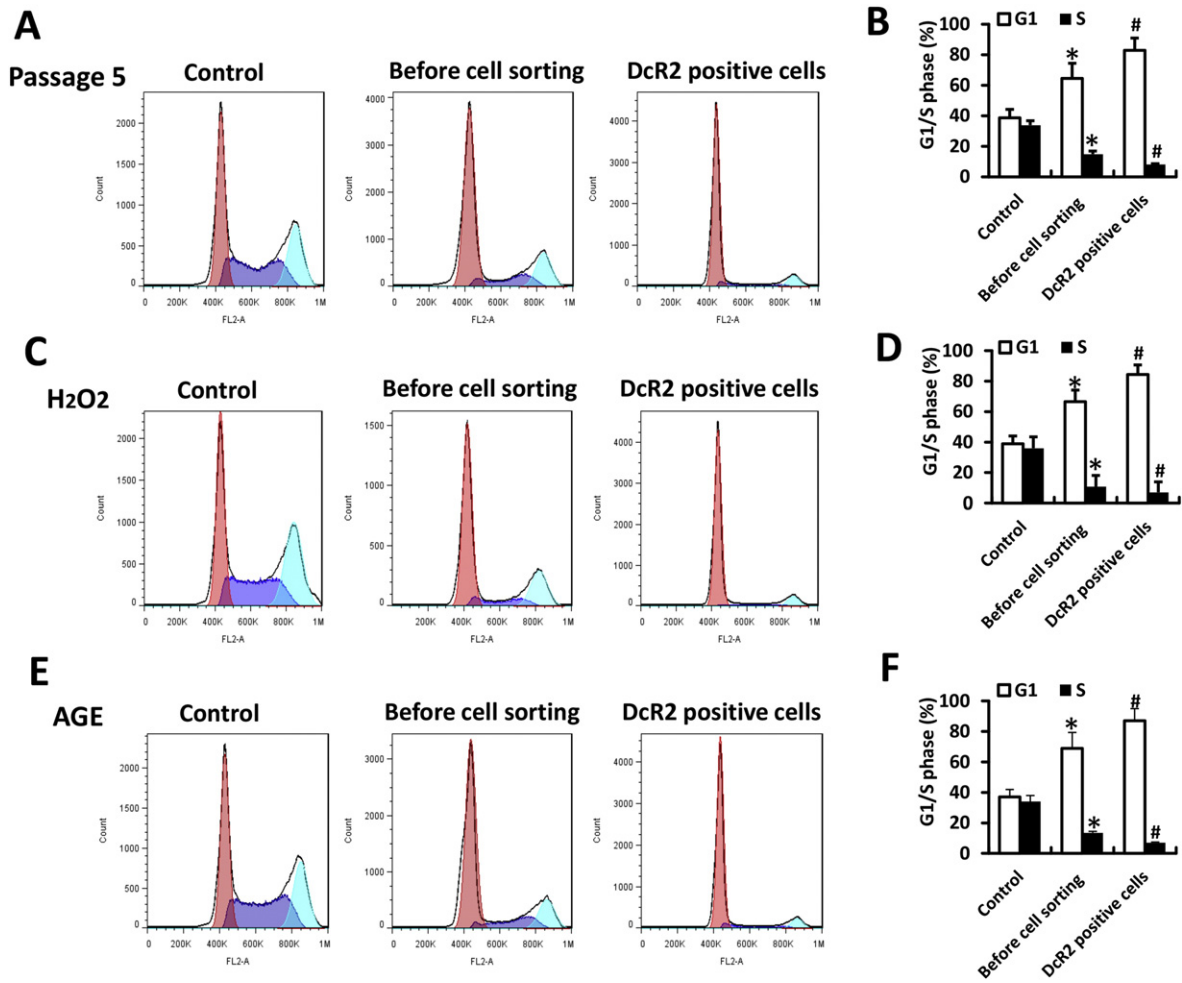


Fig. 4. Distribution of cell cycle in pre-sorted RTECs and DcR2-positive cells in each senescent model group. The percentages of cells in G1 phase on Passage 5 (A–B) and H₂O₂- (C–D) and AGEs- (E–F) induced RTECs are increased as compared to that in the control groups; S-phase percentage is lower than that in the control group. The percentage of DcR2 positive cells in G1 phase was significantly increased compared to pre-sorting levels, while those in S phase were significantly decreased. * $P < 0.05$ vs. control; # $P < 0.05$, vs. before cell sorting.

in each field of vision were examined. The percentage of SAHF-positive cells out of the total number of RTECs was calculated (Lawless et al. 2010).

2.9. ELISA for IL-6 and TGF- β 1 in the cell culture supernatant

Cell supernatants were collected from the control group, passage 5, AGEs and H₂O₂ groups. After the adherence of MACS-sorted DcR2-positive and negative cells, normal medium was added. The cell supernatant of the two groups was collected after 48 h. The levels of IL-6 and TGF- β 1 in the supernatant were measured by ELISA kit (Hengyuan, Shanghai, China), according to the manufacturer's instructions.

2.10. Statistical analysis

Data analyses were performed with statistical software SPSS 18.0 (SPSS Inc., Chicago, IL, USA). Data are presented as mean \pm Standard deviation (SD). Comparisons of continuous variables between two groups were performed using unpaired two-tailed Student's *t*-tests. Multi-group comparisons were performed with one-way Analysis of Variance (ANOVA) and Bonferroni's multiple comparison post-hoc analysis. *P*-values < 0.05 were considered indicative of statistically significant difference.

3. Results

3.1. Enhanced expression of DcR2 in old renal tissue and senescent RTECs

Immunohistochemical examination of old renal tissue was performed to assess the expression of DcR2. The positive expression of DcR2 in tubules and the expression in old renal tissue was higher than that in the young tissues (Fig. 2A). Furthermore, we established the fifth passage of RTECs and senescent RTEC models induced by AGEs and H₂O₂ (Liu et al. 2014; Satriano et al. 2010). Immunofluorescence showed positive expression of DcR2 in the cytomembrane and cytoplasm of RTECs in all senescent models. The expression of DcR2 was significantly higher than that in normal controls (Fig. 2B–C). On Western blotting, the expression of DcR2 in each model was found to be significantly greater than that in the control group (Fig. 2D–E).

3.2. Analysis of the purity and the number of DcR2 positive cells after MACS

Flow cytometric analysis was performed to assess the purity and the number of DcR2 positive cells retrieved after MACS in each senescent model. Both the percentage of cells with surface expression of DcR2 and the number of DcR2 positive cells was assessed. Almost all the retrieved cells showed positive cell surface expression of DcR2, which was an obvious increase from that observed in the pre-sorted cells (Fig. 3A–B). However, the difference in the number of DcR2-positive

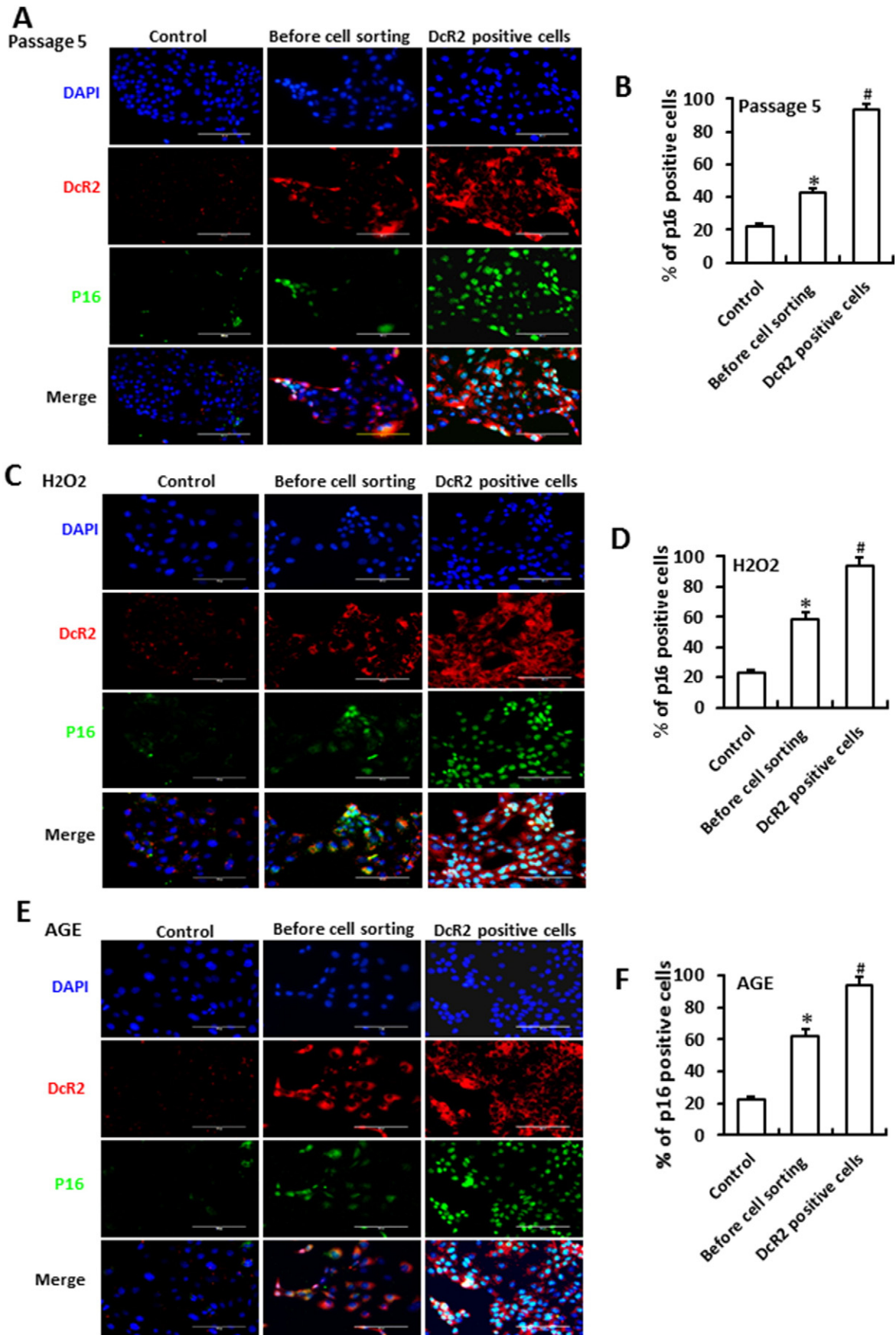


Fig. 5. SA-β-Gal staining of DcR2-positive cells before and after sorting in different senescent model groups. The percentages of SA-β-Gal positive cells on Passage 5 (A–B) and H₂O₂- (C–D) and AGEs- (E–F) induced RTECs are higher than those in control groups. The percentages of SA-β-Gal positive cells among DcR2 positive cells show a significant increase in each model group as compared to that observed prior to sorting (magnification, ×400). * *P* < 0.05 vs. control; # *P* < 0.05 vs. before cell sorting.

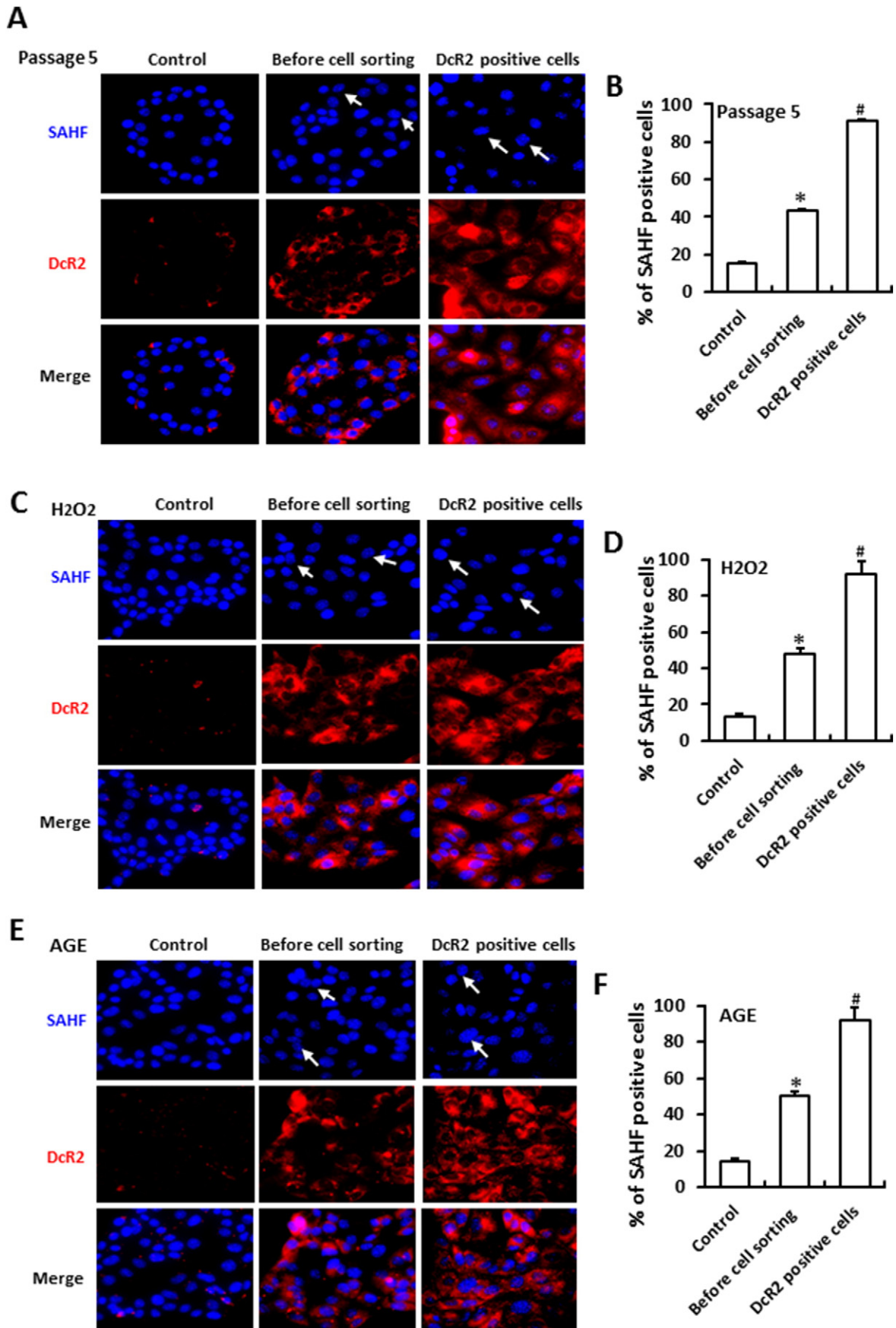


Fig. 6. p16 staining of DcR2 positive cells before and after sorting RTECs in each senescent model group. The percentages of p16 and DcR2 in Passage 5 (A–B) and H₂O₂- (C–D) and AGEs- (E–F) induced RTECs are higher than those in control groups, while the percentage of DcR2 positive cells is also greater than that in the control group. The DcR2 positive cells show high expression levels of p16 positive cells after MACS sorting; the increase from pre-sorting levels is statistically significant (magnification, $\times 400$). * $P < 0.05$ vs. control; # $P < 0.05$ vs. before cell sorting.

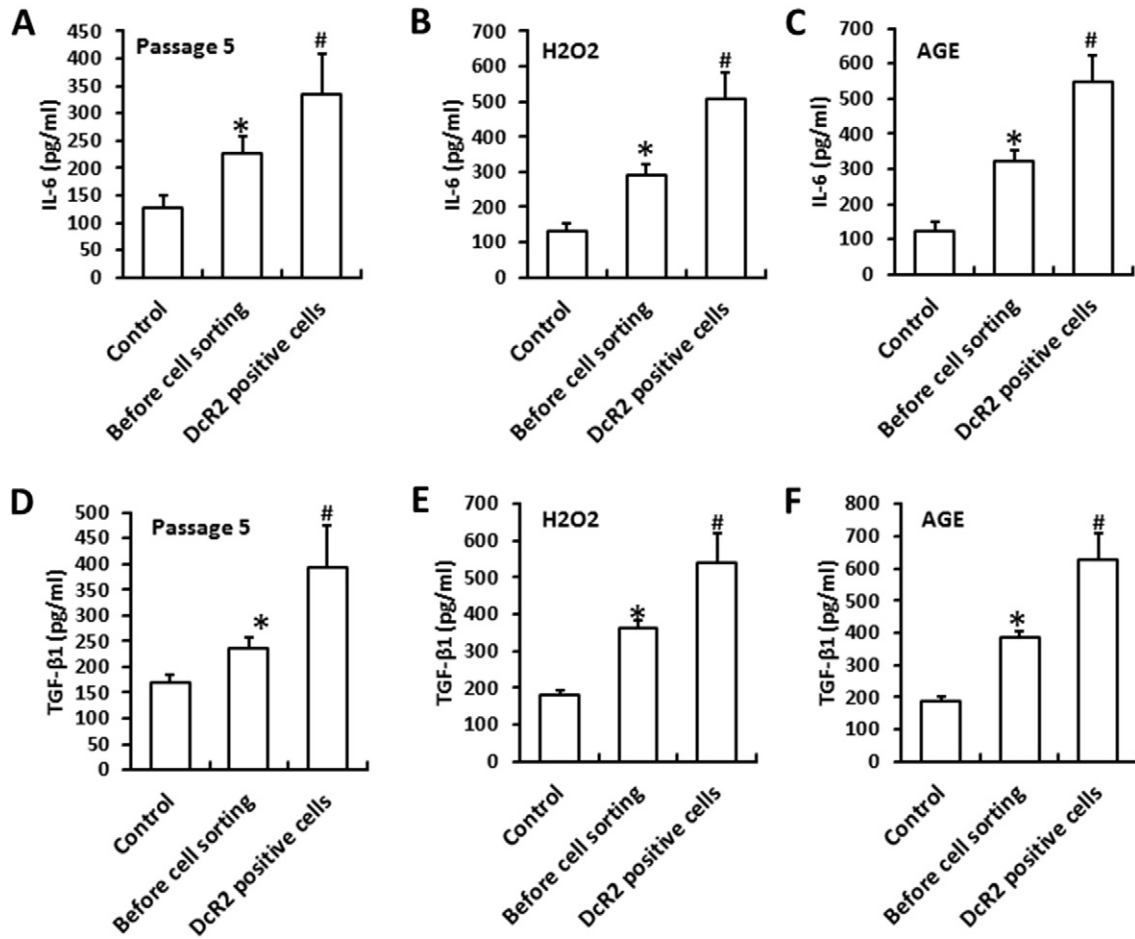


Fig. 7. SAHF staining of DcR2 positive cells before and after sorting in each senescent model group. The percentages of SAHF and DcR2 positive in Passage 5 (A–B) and H₂O₂- (C–D) and AGEs- (E–F) induced RTECs are higher than those in the control group, and a high expression of SAHF was observed in DcR2 positive cells. The percentage of SAHF positive cells in the DcR2 positive cells is significantly higher than that prior to cell sorting. The arrows represent the typical positive SAHF cells. * $P < 0.05$ vs. control; # $P < 0.05$ vs. before cell sorting.

cells between pre-sorting and after cell sorting was not statistically significant (Fig. 3C). This indicated that a large number of high purity DcR2-positive cells could be obtained by this method.

3.3. Increased percentage of cells in G1-phase and decreased percentage of cells in S-phase among the DcR2 positive RTECs

The cell cycle was arrested in G1 phase after senescence (Carnero 2013). On flow cytometric analysis, the percentage of cells in G1 phase among cells of passage 5 and AGEs- and H₂O₂- induced RTECs was greater than that in the control group, while the percentage of cells in S-phase was lower than that in the control group. Among the DcR2-positive cells obtained from MACS-derived senescent cell models, the percentage of cells in G1 phase increased by >20%, while the percentage of cells in S phase decreased by <4% from pre-sorting levels. Each senescent model cell was subjected to cell sorting at least 3 times. The standard deviation of the mean percentage of cells in the G1 and S phase was 8% and 0.5%, respectively (Fig. 4).

3.4. Enhanced expression of senescence markers in DcR2 positive RTECs

A high expression of senescence markers, SA-β-gal, p16 and senescence-related heterochromatin aggregation (SAHF) was observed in senescent cells (Carnero 2013). Positive expression of SA-β-gal was identified by blue colored cytoplasm, while positive expressions of p16 and SAHF was identified by the point-like heterochromatin structure in the nucleus. The percentages of these marker-positive cells in passage 5 and AGEs, H₂O₂ induced RTEC senescent models were higher

than those in the control group. The percentage of SA-β-gal positive cells in the DcR2-positive cells was increased by about 40% as compared to that in the senescent models prior to sorting. Each senescent model cell was subjected to cell sorting at least 3 times (Fig. 5). The percentage of p16-positive cells in the DcR2-positive cells was about 30% higher than that in the senescent cells prior to sorting (Fig. 6). The percentage of SAHF positive cells was 45% higher than that in the senescent model cells prior to sorting (Fig. 7).

3.5. Elevated levels of IL-6 and TGF-β1 in DcR2-positive RTECs

SASP after cell senescence include inflammatory factors, growth factors and chemokines (Salama et al. 2014). The levels of IL-6 and TGF-β1 in the supernatant of passage 5 and AGEs, H₂O₂ induced RTEC senescence models were higher than those in the control group. The levels of IL-6 and TGF-β1 in the supernatant of DcR2-positive cells were increased by at least 1.7 and 1.5 times as compared with those in the pre-sorted model cells (Fig. 8).

3.6. Good cell viability and poor proliferation of DcR2 positive RTECs

We also examined the adherence and proliferation of DcR2 positive and negative RTECs to rule out the effect of MACS on cell viability. The cell morphology and counts was documented at days 1, 3 and 5 post-inoculation. DcR2-positive RTECs showed no significant increase in the number of cells after 5 days of continuous culture. No significant number of floating dead cells were found. DcR2-negative RTECs showed a cobblestone configuration; the number of cells showed an exponential

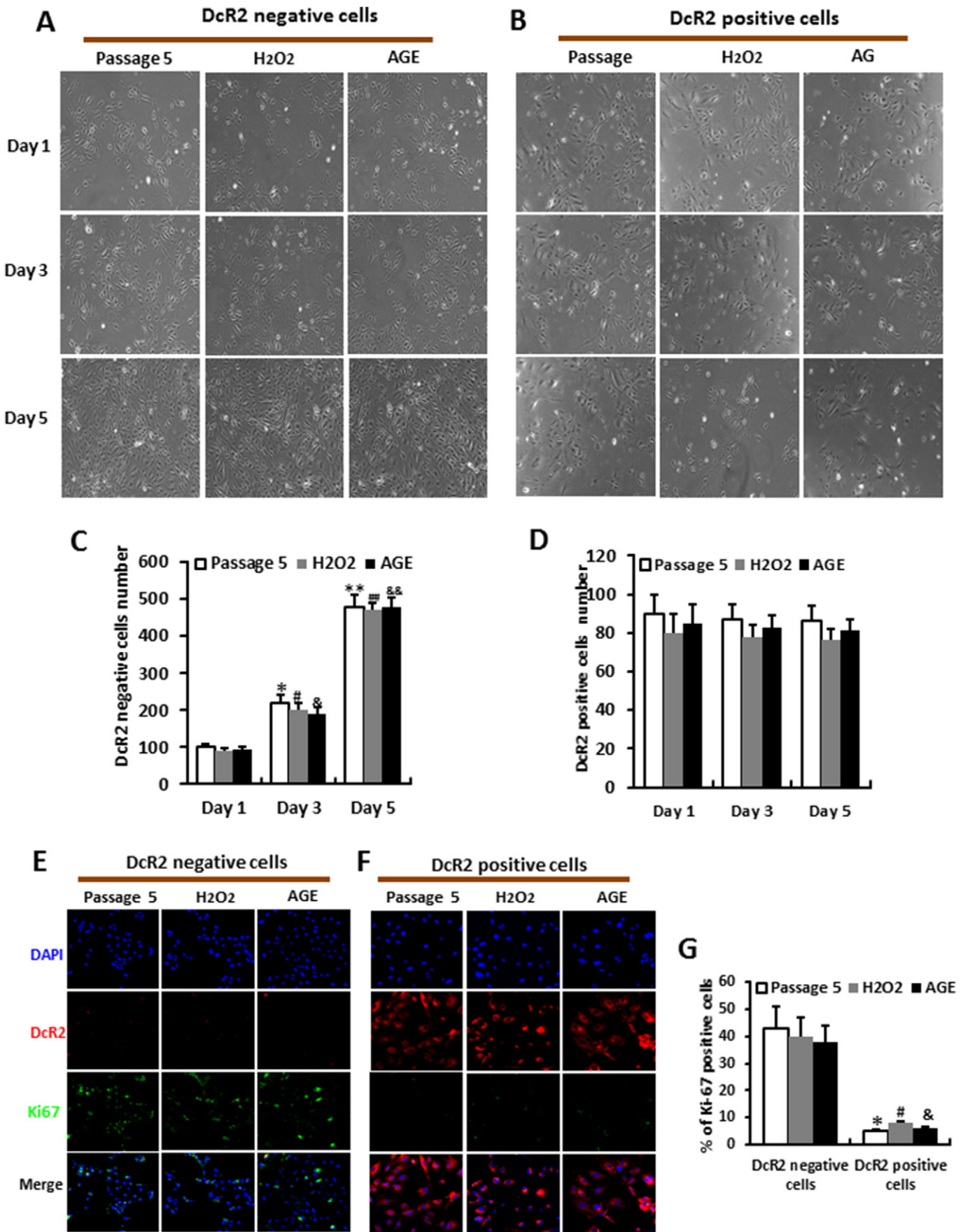


Fig. 8. The levels of IL-6 and TGF-β1 in the supernatant of pre-sorted RTECs and DcR2 positive cells in each senescent model group. The levels of IL-6 and TGF-β1 in the supernatant of Passage 5 (A, D), H₂O₂- (B, E), and AGE- (C, F) induced RTECs are higher than those in the control group, and the levels of IL-6 and TGF-β1 in the supernatant of the DcR2 positive cells are significantly higher than those in the model group prior to sorting. * $P < 0.05$ vs. control; # $P < 0.05$ vs. before cell sorting.

increase after 5 days (Fig. 9A–B). Immunofluorescence staining showed a low expression of proliferation marker Ki-67 in the DcR2-positive RTECs both before and after cell sorting, and which was at least 5-fold inferior to that of DcR2-negative cells (Fig. 9C–F). The above results indicated that DcR2-positive RTECs obtained by MACS were viable, but with no proliferative ability, while DcR2-negative RTECs had a stronger proliferative capacity than that of DcR2-positive RTECs. Furthermore, we found overexpression of anti-apoptotic molecule FLIP, but no expression or low expression of the pro-apoptotic caspase-3 in the

DcR2-positive cells, which possessed an anti-apoptotic phenotype (Fig. 9G).

4. Discussion

CKD has been used as a clinical model of cellular senescence (Stenvinkel and Larsson 2013). Renal parenchymal cell senescence model represents the typical histological changes of CKD, such as that in diabetic nephropathy, IgA nephropathy, and kidney diseases in the

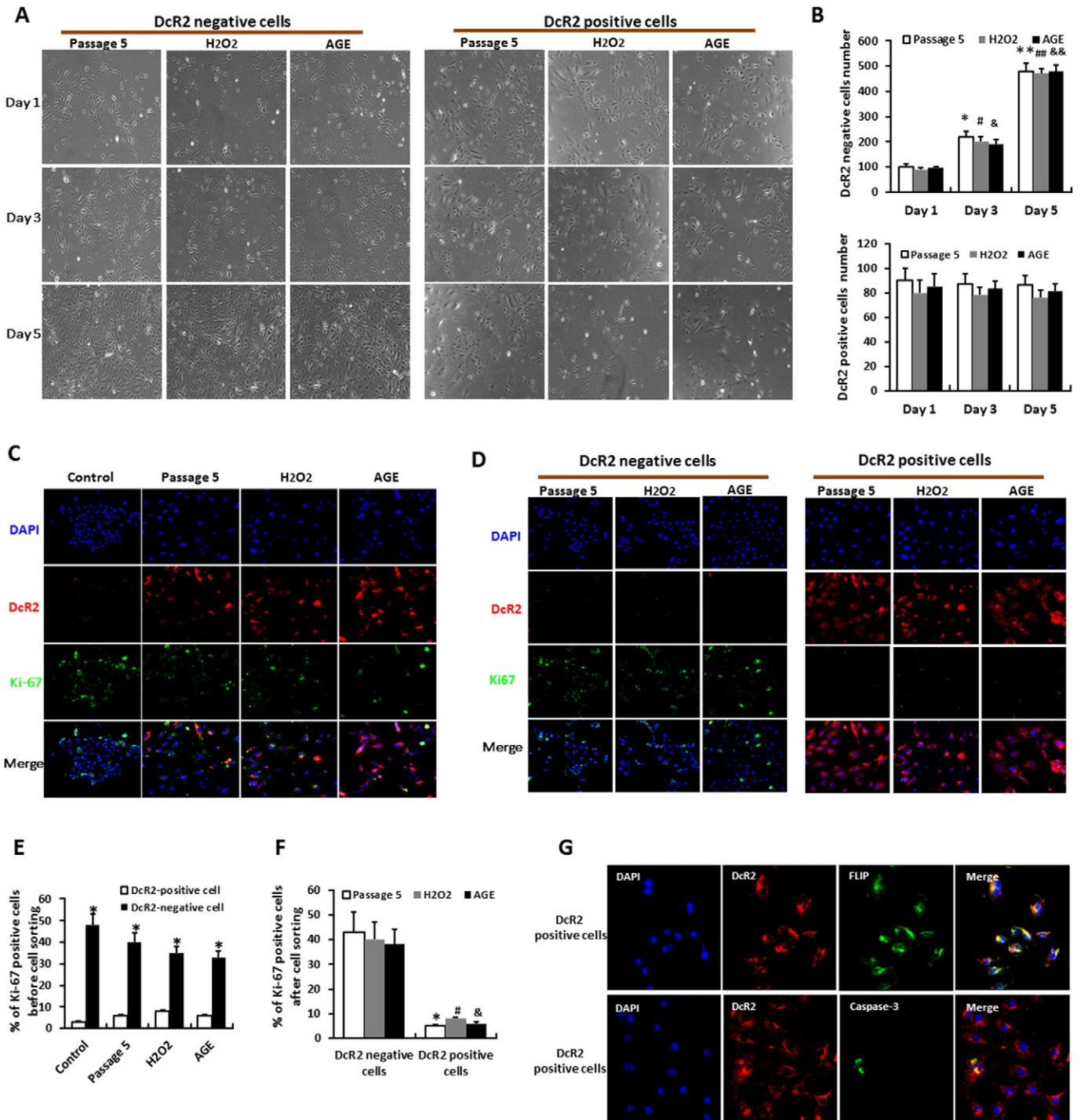


Fig. 9. Viability and proliferative ability of DcR2-positive and -negative RTECs before and after MACS in each model group. DcR2-negative RTECs increased significantly at 1, 3, and 5 days. (A–B); no significant increase in DcR2-positive RTECs were seen at 1, 3, and 5 days, and no significant dead cells were seen (magnification, $\times 100$). *^{##}: $P < 0.05$ vs. Day 1, **^{##}: $P < 0.05$ vs. Day 3. (C–F) The expression of Ki-67 in each senescent model group is higher than that in the control; DcR2-negative RTECs are significantly higher than the DcR2-positive RTECs (magnification, $\times 400$). *^{##}: $P < 0.05$ vs. DcR2 negative cells. (G) Expressions of FLIP and caspase-3 in DcR2-positive cells.

elderly (Liu et al. 2012; Satriano et al. 2010; Sis et al. 2007; Verzola et al. 2008; Yang and Fogo 2010). RTECs, rich in mitochondria, are most prone to senescence on exposure to AGEs, oxidative stress and other stimuli (Lopez-Otin et al. 2013; Youle and van der Bliek 2012). The degree of RTEC senescence in CKD is closely related to tubular atrophy, interstitial fibrosis, and degree of glomerulosclerosis, and plays a major role in the progression of CKD (Liu et al. 2012; Verzola et al. 2008). Therefore, senescent RTEC is an important model for the study of the progression of CKD. In this study, DcR2-positive cells were sorted from the fifth passage and AGEs- and H₂O₂-induced RTEC senescent models established using the MACS-specific senescent-specific marker DcR2, which demonstrated that DcR2 positive cells are biologically active senescent RTECs. It is a stable and feasible method to sort active senescent RTECs based on DcR2.

Cell senescence refers to the irreversible cell cycle arrest in G1 phase, a condition associated with high expressions of SA- β -gal in the cytoplasm and those of p16, SAHF and other senescent markers in the nucleus (Carnero 2013). The currently used method for sorting of senescent cells (FACS) employs the use of overhead markers of senescence in cell rupture conditions, and thus is not a source of live senescent cells (Hewitt et al. 2013). The other method to acquire live senescent cells is based on cell size with use of a microfluidic filter; however, the cell purity and specificity of this method is unsatisfactory (Kim et al. 2015). The transmembrane molecule DcR2 was used as a senescent marker for tumor cells in a recent study (Collado et al. 2005). In the present study, we demonstrated for the first time that DcR2 is highly expressed in the cytomembrane and cytoplasm of renal tubular cells in old kidney and passage 5, AGEs-, H₂O₂-induced RTEC senescence models. Our findings indicate that DcR2 may be a new target molecule used for isolation of live RTECs. While the high-pressure conditions in FACS are detrimental to the viability of isolated cells, MACS offers a distinct advantage in this respect.

MACS is based on binding of cell membrane markers with specific immunomagnetic beads, which results in a high yield of purely senescent cells. The high expression of senescent cell-specific phenotypes (SA- β -gal, p16, and SAHF) in the isolated DcR2-positive cells confirmed the high-specificity of MACS. We further demonstrated that the DcR2-positive cells had good cell viability but lacked proliferative ability. We also evaluated the DcR2-negative cell activity and proliferation to exclude any potential effect of MACS on cell activity and found that it was almost no influence on the biology of isolated cells. Further, the numbers of DcR2 positive cells isolated were not statistically different from the pre-sorting levels, which indicates that DcR2 antibody binding to cells did not significantly promote cell senescence. In this study, experiments with each senescent model were repeated >3 times, and the DcR2 positive cells obtained in each sorting were found to be pure active senescent RTECs. The difference between the groups was insignificant, which indicates that it is a feasible and technically sound method for sorting senescent RTECs with excellent reproducibility.

Senescent cells can secrete inflammatory factors, chemokines, and other senescence-related phenotypes, which not only promote normal peripheral cell senescence, but also induce tissue fibrosis and dysfunction (Freund et al. 2010; Salama et al. 2014). We found increased levels of IL-6 and TGF- β 1 in the 5th passage, H₂O₂ and AGEs-induced RTEC senescence models, while IL-6 and TGF- β 1 in the DcR2-positive senescent RTECs supernatant obtained by MACS sorting were higher than those of non-sorted cells. This indicates that the effect of purified senescent RTECs was not consistent with the mixed cell population prior to sorting. Senescent RTECs can be isolated and purified for more accurate and in-depth study of the progression of renal disease. Previous studies on the mechanism of senescent RTECs were performed in mixed cell populations which included other damaged and normal cells in addition to the senescent cells. Presence of cells with positive expression of markers of epithelial-mesenchymal transition, apoptosis and other forms of cell injury among AGE-induced senescent RTECs does not imply that the mechanism of cell injury is senescent RTEC-specific

(Burns et al. 2006; Maeda et al. 2013). Therefore, we used DcR2 to isolate active senescent RTECs using MACS. Our work lays the foundation for further studies on cell senescence and its role in disease progression.

A highly-pure population of DcR2-positive RTECs was isolated by MACS, which was confirmed to comprise of active senescent RTECs based on the cell cycle phase, demonstration of senescent phenotypes, and their adherent and proliferative abilities. Although this study was confined only to isolation of senescent RTECs, our work provides the basis for future research into pathogenesis of chronic kidney disease using a highly specific and reproducible method for isolation of senescent RTECs based on DcR2. The relationship between DcR2 and senescent RTEC needs to be further clarified in a follow-up study. The successful sorting of senescent active RTECs also opens the field for the development of new targeted therapies for senescent RTECs.

Conflict of interest

All authors declared that there were no conflicts of interest involved.

Acknowledgements

This study was supported by the National Natural Science Foundation of China (81470962, 81400733); the National Science and Technology Support Plan (No. 2013BAI09B05); the National Science and Technology Support Plan (No. 2015BAI12B06) and 12th Five-year National Science Technology Support Plan (No. 2011BAI10B08).

References

- Burns, W.C., Twigg, S.M., Forbes, J.M., Pete, J., Tikellis, C., Thallas-Bonke, V., Thomas, M.C., Cooper, M.E., Kantharidis, P., 2006. Connective tissue growth factor plays an important role in advanced glycation end product-induced tubular epithelial-to-mesenchymal transition: implications for diabetic renal disease. *Journal of the American Society of Nephrology*: JASN 17, 2484–2494.
- Carnero, A., 2013. Markers of cellular senescence. *Methods Mol. Biol.* 965, 63–81.
- Collado, M., Gil, J., Efeyan, A., Guerra, C., Schuhmacher, A.J., Barradas, M., Benguria, A., Zaballos, A., Flores, J.M., Barbacid, M., Beach, D., Serrano, M., 2005. Tumour biology: senescence in premalignant tumours. *Nature* 436, 642.
- Freund, A., Orjalo, A.V., Desprez, P.Y., Campisi, J., 2010. Inflammatory networks during cellular senescence: causes and consequences. *Trends Mol. Med.* 16, 238–246.
- Harper, S., 2014. Economic and social implications of aging societies. *Science* 346, 587–591.
- Hayflick, L., 1965. The limited in vitro lifetime of human diploid cell strains. *Exp. Cell Res.* 37, 614–636.
- Hewitt, G., von Zglinicki, T., Passos, J.F., 2013. Cell sorting of young and senescent cells. *Methods Mol. Biol.* 1048, 31–47.
- Kim, M.S., Jo, S., Park, J.T., Shin, H.Y., Kim, S.S., Gurel, O., Park, S.C., 2015. Method to purify and analyze heterogeneous senescent cell populations using a microfluidic filter with uniform fluidic profile. *Anal. Chem.* 87, 9584–9588.
- Kimberley, F.C., Sreaton, G.R., 2004. Following a TRAIL: update on a ligand and its five receptors. *Cell Res.* 14, 359–372.
- Lawless, C., Wang, C., Jurk, D., Merz, A., Zglinicki, T., Passos, J.F., 2010. Quantitative assessment of markers for cell senescence. *Exp. Gerontol.* 45, 772–778.
- Liu, J., Yang, J.R., He, Y.N., Cai, G.Y., Zhang, J.G., Lin, L.R., Zhan, J., Zhang, J.H., Xiao, H.S., 2012. Accelerated senescence of renal tubular epithelial cells is associated with disease progression of patients with immunoglobulin A (IgA) nephropathy. *Translational research: the journal of laboratory and clinical medicine* 159, 454–463.
- Liu, J., Huang, K., Cai, G.Y., Chen, X.M., Yang, J.R., Lin, L.R., Yang, J., Huo, B.G., Zhan, J., He, Y.N., 2014. Receptor for advanced glycation end-products promotes premature senescence of proximal tubular epithelial cells via activation of endoplasmic reticulum stress-dependent p21 signaling. *Cell. Signal.* 26, 110–121.
- Lopez-Otin, C., Blasco, M.A., Partridge, L., Serrano, M., Kroemer, G., 2013. The hallmarks of aging. *Cell* 153, 1194–1217.
- Macher-Goeppinger, S., Aulmann, S., Tagscherer, K.E., Wagener, N., Haferkamp, A., Penzel, R., Brauckhoff, A., Hohenfellner, M., Sykora, J., Walczak, H., Teh, B.T., Autschbach, F., Herpel, E., Schirmacher, P., Roth, W., 2009. Prognostic value of tumor necrosis factor-related apoptosis-inducing ligand (TRAIL) and TRAIL receptors in renal cell cancer. *Clinical cancer research: an official journal of the American Association for Cancer Research* 15, 650–659.
- Maeda, S., Matsui, T., Takeuchi, M., Yamagishi, S., 2013. Sodium-glucose cotransporter 2-mediated oxidative stress augments advanced glycation end products-induced tubular cell apoptosis. *Diabetes Metab. Res. Rev.* 29, 406–412.
- Matjusaitis, M., Chin, G., Sarnoski, E., Stolzing, A., 2016. Biomarkers to identify and isolate senescent cells. *Ageing Res. Rev.*
- Munoz-Espin, D., Serrano, M., 2014. Cellular senescence: from physiology to pathology. *Nat. Rev. Mol. Cell Biol.* 15, 482–496.

- Sagiv, A., Biran, A., Yon, M., Simon, J., Lowe, S.W., Krizhanovsky, V., 2013. Granule exocytosis mediates immune surveillance of senescent cells. *Oncogene* 32, 1971–1977.
- Salama, R., Sadaie, M., Hoare, M., Narita, M., 2014. Cellular senescence and its effector programs. *Genes Dev.* 28, 99–114.
- Satriano, J., Mansoury, H., Deng, A., Sharma, K., Vallon, V., Blantz, R.C., Thomson, S.C., 2010. Transition of kidney tubule cells to a senescent phenotype in early experimental diabetes. *Am. J. Physiol. Cell Physiol.* 299, C374–C380.
- Sis, B., Tasanarong, A., Khoshjou, F., Dadras, F., Solez, K., Halloran, P.F., 2007. Accelerated expression of senescence associated cell cycle inhibitor p16INK4A in kidneys with glomerular disease. *Kidney Int.* 71, 218–226.
- Stenvinkel, P., Larsson, T.E., 2013. Chronic kidney disease: a clinical model of premature aging. *American journal of kidney diseases: the official journal of the National Kidney Foundation* 62, 339–351.
- Terry, S., Jouret, F., Vandenabeele, F., Smolders, I., Moreels, M., Devuyt, O., Steels, P., Van Kerkhove, E., 2007. A primary culture of mouse proximal tubular cells, established on collagen-coated membranes. *Am. J. Physiol. Ren. Physiol.* 293, F476–F485.
- Verzola, D., Gandolfo, M.T., Gaetani, G., Ferraris, A., Mangerini, R., Ferrario, F., Villaggio, B., Gianiorio, F., Tosetti, F., Weiss, U., Traverso, P., Mji, M., Deferrari, G., Garibotto, G., 2008. Accelerated senescence in the kidneys of patients with type 2 diabetic nephropathy. *Am. J. Physiol. Ren. Physiol.* 295, F1563–F1573.
- Vindrieux, D., Reveiller, M., Chantepie, J., Yakoub, S., Deschildre, C., Ruffion, A., Devonec, M., Benahmed, M., Grataroli, R., 2011. Down-regulation of DcR2 sensitizes androgen-dependent prostate cancer LNCaP cells to TRAIL-induced apoptosis. *Cancer Cell Int.* 11 (42).
- Yang, H., Fogo, A.B., 2010. Cell senescence in the aging kidney. *Journal of the American Society of Nephrology: JASN* 21, 1436–1439.
- Youle, R.J., van der Bliek, A.M., 2012. Mitochondrial fission, fusion, and stress. *Science* 337, 1062–1065.
- Zhang, C., Lu, Y., Zhou, H., Lu, H., Qian, X., Liu, X., Wang, X., Ding, Z., Zhang, F., Lu, L., 2015. Acquiring Kupffer cells in mice using a MACS-based method. *Transplant. Proc.*